

Modified Eshelby tensor modeling for elastic property prediction of carbon nanotube reinforced ceramic nanocomposites

Yao Chen, Kantesh Balani, and Arvind Agarwal^{a)}

Mechanical and Materials Engineering Department, EC 3464, Florida International University, 10555 W. Flagler St., Miami, Florida 33174

(Received 16 May 2007; accepted 18 June 2007; published online 16 July 2007)

A modified model using the Eshelby equivalent tensor is developed to evaluate overall elastic properties of carbon nanotube (CNT) reinforced aluminum oxide nanocomposites. This model accounts for the effect of carbon nanotube geometry and porosity on the effective elastic modulus. Experimental results are compared with the computed predictions. Computed results show higher elastic modulus values, which are attributed to the perfect bonding between the reinforcement and the matrix. It is concluded that the modified Eshelby model can predict the elastic property of CNT reinforced ceramic nanocomposites. © 2007 American Institute of Physics.

[DOI: 10.1063/1.2756360]

Carbon nanotubes (CNTs), in the form of single-walled or multiwalled assemblies, have been the focus of considerable scientific research since the discovery of Iijima¹ due to their high elastic modulus of the order of 1000 GPa with the tensile strength in the range of 11–63 GPa,² excellent chemical stability, and excellent electrical and thermal conductivities.^{3,4} Therefore, by introducing CNTs into appropriate matrix, it is expected that the resulting composite will have largely enhanced mechanical properties compared to this unreinforced matrix. Several applications have been proposed recently for CNTs, many of which adding small amount of carbon nanotubes to ceramic to produce tougher ceramic materials.^{5–9} However, many researchers^{10–12} reported that the enhancement in the elastic modulus of carbon nanotube-based composites is lower than the expected value. Many researchers ascribed this discrepancy to inhomogeneous distribution of CNTs within the matrix, weak bonding between CNTs and matrix, and insufficient load transfer at their interface. For the fiber reinforced composites, the fibers shape, the aspect ratio, and the volume fraction significantly influence the overall elastic properties of the composites which have been modeled using micromechanics.¹³ However, dimensions of CNTs are significantly different from the conventional fiber and require modifications to the existing micromechanical models. In this research, the elastic modulus of plasma sprayed aluminum oxide reinforced with carbon nanotubes was experimentally evaluated using nanoindentation and modulus mapping. A modified model using the Eshelby equivalent tensor is developed to elucidate the effect of geometry characteristics of the carbon nanotubes and porosity on the overall elastic properties of the nanocomposite.

Spray dried nano- Al_2O_3 agglomerate with addition of 4 and 8 wt % CNTs (95 % + pure, 40–70 nm in outer diameter, and 0.5–2 mm in length) was employed as the starting powder feedstock. The plasma spraying parameters were optimized to obtain Al_2O_3 -CNT nanocomposite with improved fracture toughness, which can be referred to our previous research.¹⁴ The microstructural details were characterized by JEOL JSM 6330F field emission scanning electron micro-

copy (SEM). The porosity in plasma sprayed coatings was measured based on Archimedes' principle.¹⁵ Hysitron TriboIndenter® with a Berkovich diamond indenter tip was used to measure elastic modulus. Dynamic mechanical analysis mode (applying cyclic stress in compression at constant frequency of 200 Hz) was used to measure amplitude and phase shift of the original signal and evaluate representative storage modulus. Since plasma sprayed ceramic coatings are brittle, their stiffness could be well approximated to its storage modulus.

Figure 1 summarizes microstructure obtained in the plasma sprayed Al_2O_3 -CNT nanocomposite. It shows three main features, viz: fully melted matrix, partially melted/solid-state sintered matrix, and CNT dispersion throughout the matrix. Bimodal matrix is obtained by controlling plasma parameters to achieve: (i) melting and resolidification of the surface and (ii) solid-state sintering of the core of the spray dried agglomerate.¹⁴ Plasma sprayed aluminum oxide coating reinforced with 4 and 8 wt % CNTs is relatively dense (90.2% and 93.9%, respectively) and uniform. In addition, CNTs are uniformly distributed in the matrix owing to their typical layered structure buildup. Hence, the generated matrix microstructure and CNT dispersion influence the overall elastic modulus of nanocomposite.

To determine the longitudinal Young modulus E_{11} , it is supposed that only longitudinal normal stress is applied on the composite. Also, it is known that the average strain $\bar{\epsilon}_{11}$ of composites can be expressed as the following equation due to the presence of CNTs:¹⁶

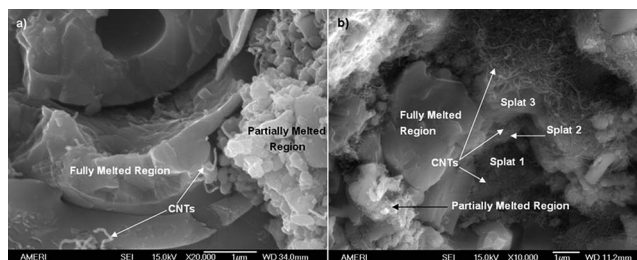


FIG. 1. SEM micrographs showing the fracture surface morphologies of plasma sprayed nanostructured aluminum oxide coating reinforced with (a) 4 wt % CNTs and (b) 8 wt % CNTs.

^{a)} Author to whom correspondence should be addressed; electronic mail: agarwala@fiu.edu

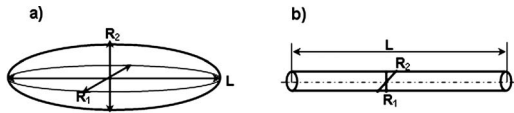


FIG. 2. Schematic illustration of (a) conventionally ellipsoidal inclusion with a primary aspect ratio $\alpha=L/R_1$ and a secondary aspect ratio $\beta=L/R_2$ and (b) three-dimensional CNT inclusion with a primary aspect ratio $\alpha=L/R_1$ and a secondary aspect ratio $\beta=L/R_2$, in which $\alpha=\beta=L/R$ ($R_1=R_2=R$, L and R are length and outer diameter of the CNT, respectively).

$$\bar{\varepsilon}_{11} = \varepsilon_{11}^m + f\varepsilon_{11}^{\text{CNT}}, \quad (1)$$

where $\bar{\varepsilon}_{11}$ is the average strain of the composite, ε_{11}^m is the strain of the pure matrix, $\varepsilon_{11}^{\text{CNT}}$ is the equivalent transformation strain resulted from the CNTs into matrix, and f is the volume fraction of the CNTs within the plasma sprayed nanocomposite. Also,

$$E_{11} = (\bar{\varepsilon}_{11})^{-1}\bar{\sigma}_{11}, \quad (2)$$

$$\bar{\sigma}_{11} = E_m\varepsilon_{11}^m. \quad (3)$$

Therefore,

$$E_{11} = E_m\varepsilon_{11}^m(\varepsilon_{11}^m + f\varepsilon_{11}^{\text{CNT}})^{-1}. \quad (4)$$

For nanocomposite including CNTs, the volume fraction of CNTs can be estimated by the density of composite constituents as follows:¹²

$$f = \frac{\rho_c}{\rho_{\text{CNT}}}w_{\text{CNT}}, \quad (5)$$

in which ρ_c , ρ_{CNT} , and w_{CNT} are density of the composite, density of CNT, and addition weight fraction of CNTs, respectively. It is well known that the microstructure of plasma sprayed coatings is characterized by the porosity. Hence, it is necessary to introduce porosity into the modified model to account for its effect on plasma sprayed CNT reinforced ceramic nanocomposite coatings. The density of composite ρ_c can be calculated by the following equation:

$$\rho_c = f\rho_{\text{CNT}} + (1 - \phi - f)\rho_m, \quad (6)$$

in which ρ_m is the density of the matrix.

The equivalent transformation strain $\varepsilon_{11}^{\text{CNT}}$ can be obtained from matrix M_{ijkl} as follows:¹⁵

$$\begin{pmatrix} M_{1111} & M_{1122} & M_{1133} \\ M_{2211} & M_{2222} & M_{2233} \\ M_{3311} & M_{3322} & M_{3333} \end{pmatrix} \begin{pmatrix} \varepsilon_{11}^{\text{CNT}} \\ \varepsilon_{22}^{\text{CNT}} \\ \varepsilon_{33}^{\text{CNT}} \end{pmatrix} = \begin{pmatrix} M_{11} \\ M_{22} \\ M_{33} \end{pmatrix}, \quad (7)$$

in which M_{ijkl} such as M_{1111} , M_{1122} , M_{1133} , M_{2211} , M_{2222} , M_{2233} , M_{3311} , M_{3322} , M_{3333} , M_{11} , M_{22} , and M_{33} can be expressed as functions of f , Eshelby's tensor S_{ijkl} , which are referred to Ref. 16 and D_1 , D_2 , and D_3 , which can be expressed as a function of Lamé's constant of matrix and CNT.¹⁶ It is supposed that only longitudinal normal σ_{11} is applied to the nanocomposite because longitudinal modulus E_{11} of the composites is the focus of this study. Therefore, $\varepsilon_{22}^{\text{CNT}}$ and $\varepsilon_{33}^{\text{CNT}}$ can be assumed to be zero. Eshelby's tensor S_{ijkl} is dependent on the aspect ratio α and β for the inclusion and Poisson's ratio of the matrix ν_m , and they can be derived from the explicit expressions of Mura.¹⁷

The primary aspect ratio α and secondary aspect ratio β of ellipsoidal inclusion for Eshelby's model are defined in Fig. 2(a). Similarly, the geometry characteristics of CNT are

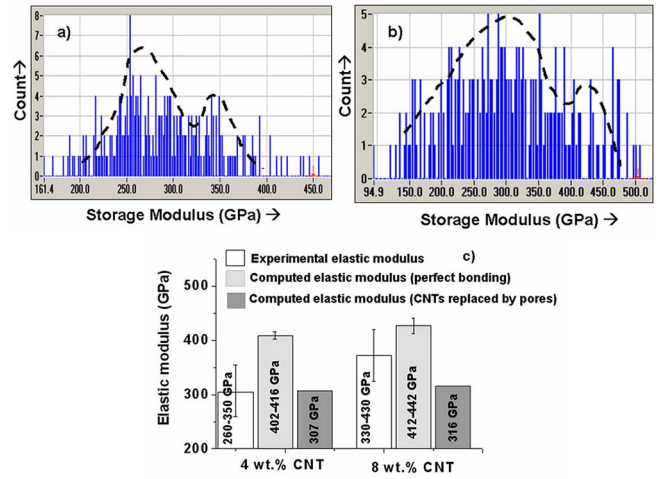


FIG. 3. Elastic modulus mapping of (a) 4 wt % CNT reinforced aluminum oxide nanocomposite and (b) 8 wt % CNT reinforced aluminum oxide nanocomposite, and (c) comparison with experimental and computed elastic moduli of both nanocomposites.

also expressed by primary aspect ratio α and secondary aspect ratio β , as shown in Fig. 2(b). It is clearly seen that for the cylindrical CNTs, the primary aspect ratio and the secondary aspect ratio are same. According to the following equation:¹⁶

$$\theta = \sin^{-1}\left(1 - \frac{R_2^2}{L^2}\right)^{1/2}, \quad (8)$$

in which R_2 and L are diameter and length of CNTs, respectively. It is clearly seen that R_2/L is very small for CNTs, leading to the fact that θ is approximately $\pi/2$, which will be used to calculate the Eshelby tensor S_{ijkl} . In this research, $\rho_{\text{CNT}}=2.25 \text{ g/cm}^3$, $\rho_m=\rho_{\text{Al}_2\text{O}_3}=3.96 \text{ g/cm}^3$, $E_{\text{CNT}}=600-1000 \text{ GPa}$, $E_{\text{Al}_2\text{O}_3}=390 \text{ GPa}$, $\nu_{\text{CNT}}=0.18$, $\nu_{\text{Al}_2\text{O}_3}=0.22$ are employed for computation. Also, two different sizes of CNTs with $L_{\text{CNT}}=500 \text{ nm}$, $R_{\text{CNT}}=40 \text{ nm}$ and $L_{\text{CNT}}=2000 \text{ nm}$, $R_{\text{CNT}}=70$ are taken into account in simulation. The overall elastic modulus is computed as 402–416 GPa for 4 wt % CNT reinforced aluminum oxide nanocomposite and 412–442 GPa for 8 wt % reinforced aluminum oxide nanocomposite, respectively. The experimental values of elastic modulus are 260–350 GPa for 4 wt % CNT reinforced aluminum oxide composite and 330–430 GPa for 8 wt % reinforced aluminum oxide composite, respectively [Figs. 3(a) and 3(b)]. It is clearly seen that computed elastic modulus of CNT reinforced aluminum oxide composites is higher, and the discrepancy between computed and experimental elastic moduli is $\sim 36\%$ for 4 wt % CNT reinforced aluminum oxide composite and $\sim 14\%$ for 8 wt % reinforced aluminum oxide composite, respectively [Fig. 3(c)]. In order to further validate the modified Eshelby model, another calculation is done by replacing the CNTs with empty pores of exact dimension. The results are 307 GPa (lower than the upper limit of experimental value) for 4 wt % CNTs replaced with pores and 315 GPa (lower than the lower limit of experimental value) for 8 wt % CNTs replaced with pores, as shown in Fig. 3(c). The results illustrate that bonding between CNT and matrix contributes to discrepancy between simulated and measured values. It should be noted that the Eshelby model assumes a perfect bonding between reinforcement and matrix.

On the other hand, the lower experimental value of the effective elastic modulus of the plasma sprayed CNT reinforced aluminum oxide is also attributed to the layered splat structure and weak bonding between the splats.¹⁸ It is well known that plasma deposited splats are often characterized by intersplat pores, cracks, and fine voids leading to inadequate bond strength between the splats, and the splats within as-sprayed coating are often held together by mechanical interlocking. Therefore, when a load is applied to the as-sprayed coating, splat sliding results in macrodeformation at splat boundaries and subsequently lowers the elastic modulus, which is the main reason for discrepancy between experimental and computed elastic moduli. The discrepancy between the experimental and computed values is lower (14%) for 8 wt % reinforced aluminum oxide nanocomposite which has been attributed to the distribution of higher CNT content in plasma sprayed coating. It is evident from Fig. 1(b) that higher amount of CNTs are distributed between successive splat boundaries. CNTs between the splats serve as the pinning agent and reduce the splat sliding due to their high strength. Due to lower CNT content in 4 wt % nanocomposite, the splat sliding is higher which leads to lower values of experimental elastic modulus.

In conclusion, a modified Eshelby tensor model, in which the geometry characteristics of CNTs and porosity are taken into account, is developed to evaluate the overall elastic properties of plasma sprayed CNT reinforced aluminum oxide nanocomposite. The simulated elastic modulus is higher than the experimental value, which is largely attributed to inadequate bond strength between splats, splat sliding and perfect bonding between CNTs and matrix assumed in Eshelby's model. The results illustrate that the modified model can be employed to predict the elastic properties of nanocomposites reinforced with CNTs.

The authors would like to acknowledge the financial support received from the Office of Naval Research (N00014-05-1-0398) and DURIP (N00014-06-0675) to perform this work. One of the authors (K.B.) also acknowledges Dissertation Year Fellowship from the Florida International University.

- ¹S. Iijima, *Nature (London)* **354**, 56 (1991).
- ²M. F. Yu, O. Lourie, M. J. Dyer, K. Moloni, T. F. Kelly, and R. S. Ruoff, *Science* **287**, 637 (2000).
- ³I. Alexandron, E. Kymakis, and G. A. J. Amaratunga, *Appl. Phys. Lett.* **80**, 1435 (2002).
- ⁴M. J. Biercuk, M. C. Liaguno, M. Radosavljevic, K. K. Hyun, A. T. Johnson, and J. E. Fischer, *Appl. Phys. Lett.* **80**, 2767 (2002).
- ⁵G. D. Zhang, J. D. Kuntz, J. L. Wan, and A. K. Mukherjee, *Nat. Mater.* **2**, 38 (2003).
- ⁶X. Wang, N. P. Padture, and H. Tanaka, *Nat. Mater.* **3**, 539 (2004).
- ⁷R. H. Baughman, A. A. Zakhidov, and W. A. de Heer, *Science* **297**, 787 (2002).
- ⁸E. T. Thostenson, Z. F. Ren, and T. W. Chou, *Compos. Sci. Technol.* **61**, 1899 (2001).
- ⁹K. Balani, R. Anderson, T. Laha, M. Andara, J. Tercero, E. Crumpler, and A. Agarwal, *Biomaterials* **28**, 618 (2007).
- ¹⁰D. Qiao, E. C. Dickey, R. Andrews, and T. Rantell, *Appl. Phys. Lett.* **76**, 2868 (2000).
- ¹¹L. S. Schadler, S. C. Giannaris, and P. M. Ajayan, *Appl. Phys. Lett.* **73**, 3842 (1998).
- ¹²E. T. Thostenson and T. W. Chou, *J. Phys. D* **36**, 573 (2003).
- ¹³S. N. Nasser and M. Hori, *Micromechanics: Overall Properties of Heterogeneous Materials* (Elsevier, New York, 1999), Vol. 2, p. 250.
- ¹⁴K. Balani, S. R. Bakshi, Y. Chen, T. Laha, and A. Agarwal, *J. Nanosci. Nanotechnol.* (in press).
- ¹⁵S. O. Chwa, D. Klein, F. L. Toma, G. Bertrand, H. Liao, C. Coddet, and Akira Ohmori, *Surf. Coat. Technol.* **194**, 215 (2005).
- ¹⁶K. Y. Lee and D. R. Paul, *Polymer* **46**, 9064 (2005).
- ¹⁷T. Mura, *Micromechanics of Defects in Solids* (Martinus Nijhoff, The Hague, 1987), Vol. 2, p. 74.
- ¹⁸F. Tang and J. M. Schoenung, *Scr. Mater.* **54**, 1587 (2006).